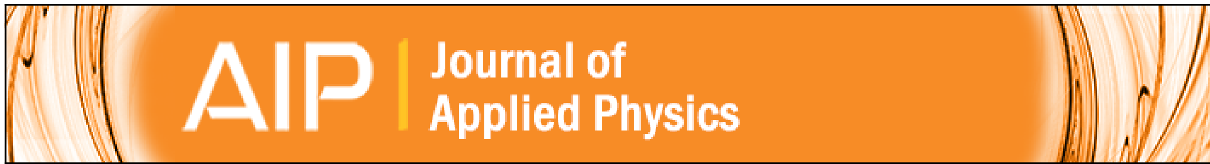

Characterization of 2.3m GaInAsSb-based vertical-cavity surface-emitting laser structures using photo-modulated reflectance

G. M. T. Chai, T. J. C. Hosea, N. E. Fox, K. Hild, A. B. Ikyo, I. P. Marko, S. J. Sweeney, A. Bachmann, S. Arafin, and M.-C. Amann

Citation: Journal of Applied Physics **115**, 013102 (2014); doi: 10.1063/1.4861146
View online: http://dx.doi.org/10.1063/1.4861146
View Table of Contents: http://scitation.aip.org/content/aip/journal/jap/115/1?ver=pdfcov
Published by the AIP Publishing

Re-register for Table of Content Alerts

Create a profile.

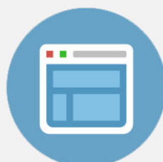

Sign up today!

[This article is copyrighted as indicated in the article. Reuse of AIP content is subject to the terms at: http://scitation.aip.org/termsconditions. Downloaded to] IP: 164.67.194.158 On: Tue, 07 Jan 2014 22:58:43

JOURNAL OF APPLIED PHYSICS 115, 013102 (2014)

Characterization of 2.3 μm GaInAsSb-based vertical-cavity surface-emitting laser structures using photo-modulated reflectance

G. M. T. Chai,[1] T. J. C. Hosea,[1,2,a)] N. E. Fox,[2] K. Hild,[2] A. B. Ikyo,[2] I. P. Marko,[2] S. J. Sweeney,[2] A. Bachmann,[3] S. Arafin,[3] and M.-C. Amann[3]
[1]*Ibnu Sina Institute for Fundamental Science Studies, Universiti Teknologi Malaysia, Johor Bahru 81310, Malaysia*
[2]*Advanced Technology Institute and Department of Physics, University of Surrey, Guildford GU2 7XH, United Kingdom*
[3]*Walter Schottky Institut, Technische Universität Munchen, Am Coulombwall 4, D-85748 Garching, Germany*

(Received 17 October 2013; accepted 17 December 2013; published online 7 January 2014)

We report angle dependent and temperature dependent (9 K–300 K) photo-modulated reflectance (PR) studies on vertical-cavity surface-emitting laser (VCSEL) structures, designed for 2.3 μm mid-infrared gas sensing applications. Changing the temperature allows us to tune the energies of the quantum well (QW) transitions relative to the VCSEL cavity mode (CM) energy. These studies show that this VCSEL structure has a QW-CM offset of 21 meV at room temperature. Consequently the QW ground-state transition comes into resonance with the CM at 220 ± 2 K. The results from these PR studies are closely compared with those obtained in a separate study of actual operating devices and show how the PR technique may be useful for device optimisation without the necessity of having first to process the wafers into working devices. © *2014 AIP Publishing LLC*.
[http://dx.doi.org/10.1063/1.4861146]

I. INTRODUCTION

A commonly used technique for mid-infrared (mid-IR) gas sensing is tunable diode laser absorption spectroscopy. Distributed feedback (DFB) lasers are currently preferred in these applications as they operate in single transverse and longitudinal modes with narrow linewidths. However, these lasers are comparatively expensive, have high power consumption, and have a highly asymmetric beam-profile requiring additional beam control optics which adds cost and complexity to the package. In contrast, vertical-cavity surface-emitting lasers (VCSELs) typically have symmetrical beam profiles making the optical system much simpler and cheaper. GaSb-based VCSELs, operating in the same mid-IR region, have single longitudinal mode operation and so could be an improved replacement for DFB lasers.[1–3] The major challenge in achieving efficient lasing in VCSELs is strongly dependent on the wavelength alignment between the peak of the gain spectrum of the active quantum well (QW) layers and the cavity mode (CM) dip in the reflectance spectrum of the VCSEL Fabry-Perot structure.[4,5] When other effects such as self-heating and non-radiative recombination have been taken into account, achieving an optimized alignment at the desired operating temperature between the energy positions of the QW ground-state transition (E_{QW}) and the CM dip in the reflectance spectrum (E_{CM}) should give improved device performance.[6] It is thus critical to know the initial E_{CM}/E_{QW} alignment especially with respect to the temperature performance of devices.[5] Therefore, it is important to be able to monitor the degree of any such misalignment, ideally prior to fabricating the devices from the as-grown VCSEL structure wafers, for example, so that optimum wafer positions can be determined for device selection. We report here on non-destructive optical spectroscopic studies of pre-fabrication 2.3 μm VCSEL wafers, in order to determine the effects of detuning the reflectance spectrum CM dip and QW ground-state transition energy, without having to process them into working devices. The technique we use, photo-modulated reflectance (PR), is well known as a powerful non-destructive, non-contact method of studying the E_{CM}/E_{QW} alignment in VCSEL structures and is unique in potentially being able to directly monitor the QW transition energies of a full VCSEL structure.[7] In devices, the degree of this alignment is often referred to as gain-cavity tuning. We use PR as function of both incident angle and temperature to study this tuning. As a comparison, and to aid our interpretation, we also use PR to study a control sample with the top VCSEL mirror removed by etching, which had been prepared for corroborative photoluminescence studies. Our conclusions from these PR studies are compared closely with the results of a separate study of the performance of operating devices made from the same wafer structures.[8]

II. SAMPLE AND EXPERIMENTAL DETAILS

Molecular beam epitaxy was used to grow two type-I GaInAsSb/AlGaAsSb/GaSb VCSEL wafers targeting emission at ~2.33 μm. The samples consist of the following layer structure: an n-doped GaSb substrate; a 24-pair n-doped bottom $AlAs_{0.09}Sb_{0.91}/GaSb$ distributed Bragg reflector (DBR) stack; five 11-nm-thick compressively strained (1.6% strain) $Ga_{0.63}In_{0.37}As_{0.11}Sb_{0.97}$ QWs, sandwiched between 8-nm-thick $Al_{0.33}Ga_{0.67}As_{0.03}Sb_{0.97}$barriers; for optical and current confinement purposes a strongly doped p+ GaSb/n+ InAsSb buried tunnel junction (BTJ) is positioned upon the active region at a node of optical field intensity; and finally a top DBR stack of a Si/SiO_2.[8,9] Full details of the growth and

a)Author to whom correspondence should be addressed. Electronic mail: j.hosea@surrey.ac.uk

 © 2014 AIP Publishing LLC

[This article is copyrighted as indicated in the article. Reuse of AIP content is subject to the terms at: http://scitation.aip.org/termsconditions. Downloaded to] IP: 164.67.194.158 On: Tue, 07 Jan 2014 22:58:43

structure are given in Ref. 9. Having a BTJ as a current aperture in the structure improves current injection, the aim being to reduce resistive heating and absorption loss within the VCSEL, because n-doped material has lower free carrier absorption and a higher electrical conductivity.[1] Despite the structural improvement with the BTJ design, it was found that, at room temperature, this device had a threshold current density of 2.5 kA/cm^2, a differential efficiency of 2%, and a maximum power output of 87 μW (at a current of $\approx$14 mA and voltage $\approx$1.4 V).[9] As commented on by the authors of Ref. 9 this performance might be contributed to by a significant unintentional detuning between the position of CM energy, E_{CM}, and ground-state QW transition energy, E_{QW}. In order to check this we used PR to investigate in detail the relative alignment of these two energies. The lasing wavelength can also be strongly affected by the growth conditions and in the present case it varied across the 2.5 cm radius of the wafer, due to a 25 nm blue shift in E_{CM} from the wafer centre to its edge. Two samples were studied here: sample A is a strip from the centre to the edge of the full VCSEL structure wafer; sample B was taken from the edge of the aforementioned etched wafer with the top DBR layer removed.

As proposed in Ref. 7, temperature-variation PR spectroscopy was used to characterize both samples. PR is well known as a non-destructive, contactless, and yet most sensitive spectroscopic technique. In essence PR externally modulates the complex dielectric function, $\varepsilon_1 + i\varepsilon_2$, of the sample using a chopped laser pump source which in turn modulates the sample reflectivity R. Since one normally measures R and ΔR simultaneously in PR, then in VCSEL structures PR can give not only a direct determination of E_{CM} from the R spectrum, but may also allow the QW ground-state transition energy E_{QW} to be measured, or inferred by varying some external parameter, thus revealing the extent of alignment of E_{CM} and E_{QW}—an attribute very important to successful device operation.[7]

To establish the basic optical characteristics of the samples, a series of room temperature (RT) reflectivity spectra were measured on sample A as a function of incidence angle, θ, ranging from 21° to 85° using a single-grating spectrometer, tungsten filament lamp, lock-in amplifier and cooled InSb detector. A mechanical chopper set at 333 Hz was placed in front of the spectrometer exit slit. By chopping the light that was to be reflected off the sample it was then possible to use lock-in amplification to detect the sample's reflectivity with low background noise. It was important here to have high quality normalised reflectivity measurements for the VCSEL structures (where by "normalised" we mean the removal of the effects of the spectral response of the measuring system, i.e., the "system response"). To measure the system response, the samples were substituted with an aluminium mirror and the reflectivity again measured under the same conditions (at RT only). The system response could then be obtained by dividing the mirror's measured reflectivity by its known reflectivity curve (provided by the manufacturer). Dividing the measured reflection spectra of the samples by this system response then yielded the desired normalised reflectivity spectra for the samples.

For the temperature variation PR measurements, the experimental set-up was similar to that described in Ref. 7 with the samples held in a closed-cycle helium cryostat for later cooling but at a fixed incidence angle of 45° ± 5°. The samples were modulated with an 808 nm, 450 mW GaAlAs diode laser electrically chopped at 812 Hz. The samples were cooled down to 9 K, and a sequence of PR spectra was measured up to RT using the same spectrometer, detector, and lock-in arrangement described above for the angle-dependent R measurements, but without the chopper in front of the spectrometer exit slit.

III. THEORETICAL BACKGROUND

In PR, the AC component of the reflectivity, ΔR, generally has a sharp derivative-like form whose energy-positions reveal the sample's electronic transition energies; uninteresting broad backgrounds in R are removed. When the laser is on, carriers are excited, drift in the built-in electric field and get trapped in various centres, which in turn decreases the field. When the laser is off, the carriers are released from the traps, and the field is restored to its original value. This mechanism of modulating internal electric fields gives periodic changes in the sample's complex dielectric function, $\delta\varepsilon_1 + i\delta\varepsilon_2$ and, thus, yield the relative changes in reflectivity, ΔR/R, which defines the PR signal:[7,10]

$$\frac{\Delta R}{R} = \alpha\delta\varepsilon_1 + \beta\delta\varepsilon_2. \tag{1}$$

Equation (1) describes the relative changes in the sample reflectivity due to the applied oscillating electric field (via the chopped laser) where $\delta\varepsilon_1$ and $\delta\varepsilon_2$ represent the modulated QW dielectric function lineshape, given by appropriate expressions such as the Aspnes third derivative functional form (TDFF), while α and β are the Seraphin coefficients, $(\partial R/\partial\varepsilon_1)/R$ and $(\partial R/\partial\varepsilon_2)/R$, respectively. In simple heterostructures with relatively few layers the Seraphin coefficients are normally considered to be energy independent compared to $\delta\varepsilon_1$ and $\delta\varepsilon_2$ and contribute only phase information to a TDFF lineshape for Eq. (1). However, in VCSEL structures α and β are strongly varying with energy in the vicinity of any prominent features in the R spectrum, such as near the CM dip. Thus, in the case of measuring the PR of VCSEL structures, a modified form of Eq. (1) is required that allows for the energy dependence of α and β, as described in detail in Ref. 11. We will not describe this model in detail here, but, to summarise; in the vicinity of E_{CM}, α and β can essentially be assumed to result from the modulation of the effective refractive index and absorption, respectively, of the active cavity region which cause modulation changes in the cavity optical thickness (and thus E_{CM}) and CM dip depth, respectively.[11] In the vicinity of E_{QW}, $\delta\varepsilon_1$ and $\delta\varepsilon_2$ result from the modulated complex dielectric function of the QW and can, for instance, be described by a TDFF. Both pairs of parameters—$\delta\varepsilon_1$ and $\delta\varepsilon_2$, and α and β—form Kramers-Kronig pairs so that, while α has a dispersive (i.e., anti-symmetric) shape near E_{CM}, β has an absorptive (symmetric) form. In contrast, $\delta\varepsilon_1$ has an essentially absorptive (symmetric) form near E_{QW} while $\delta\varepsilon_2$ is dispersive

[This article is copyrighted as indicated in the article. Reuse of AIP content is subject to the terms at: http://scitation.aip.org/termsconditions. Downloaded to] IP: 164.67.194.158 On: Tue, 07 Jan 2014 22:58:43

(anti-symmetric).[5,7] The product of these pairs of lineshapes in Eq. (1) results in a rather complicated interplay between the symmetries and intensities of the four features. However, this can be written down in a suitable analytical form that can be used to fit the measured VCSEL PR spectra.[11]

IV. RESULTS AND DISCUSSIONS

A. Angle dependent reflectivity

In the situation where $E_{QW} > E_{CM}$ at RT and at normal incidence, it may be possible to tune E_{CM} to move into resonance with E_{QW} by increasing the angle of incidence θ of the spectrometer light being shone onto the front surface of the VCSEL structure. Increasing θ causes the CM dip to blue-shift to higher energy, whereas the QW ground-state electronic transition energy, E_{QW}, must necessarily be independent of θ. In terms of wavelengths, the behaviour of λ_{CM} with θ may be described by

$$\lambda_{CM}(\theta) = \lambda_{CM}(0^\circ)\sqrt{1 - \frac{\sin^2(\theta)}{n_{eff}^2}}, \quad (2)$$

with $\lambda_{CM}(0^\circ)$ the normal incidence CM wavelength, given by $\frac{2n_{eff}d}{m}$ with m describing the mode order of interference, d the thickness, and n_{eff} the refractive index, of the effective cavity.[7] Whether or not increasing θ can accomplish the desired crossing of E_{QW} and E_{CM} clearly depends on the total amount of blue-shift in E_{CM} accessible by this method, and the initial relative positions of E_{QW} and E_{CM} at normal incidence.

For the full VCSEL structure sample A, the RT angle dependent normalised reflectivity spectra showed the expected blue shift in the CM dip energy with increasing angle (see Fig. 1). As suggested by Eq. (2), the square of the λ_{CM} (θ) results obtained were plotted against the square of sine of θ and the results fitted to give a very satisfactory straight line fit

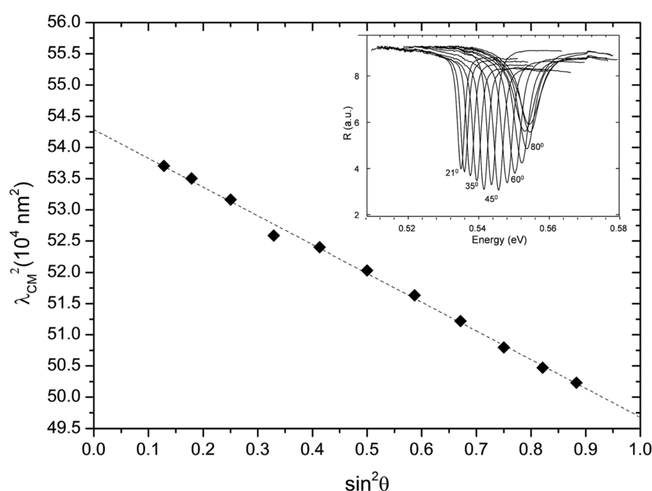

FIG. 1. The square of the VCSEL sample A cavity mode wavelength $\lambda_{CM}(\theta)$ at room temperature versus the square of the sine of incidence angle θ (solid diamonds). The dashed line is a fit with Eq. (2). The inset shows examples of the room temperature angle dependent normalised reflectivity spectra in the vicinity of the cavity mode, showing that the CM dip profile also changes with angle, the deepest most symmetric dip being observed at $\sim$0.544 eV at $\theta \approx 45^\circ \pm 5^\circ$.

(Fig. 1) with fit parameters $\lambda_{CM}(0^\circ) = 2.329 \pm 0.001\ \mu$m and $n_{eff} = 3.433 \pm 0.003$, the latter value being comparable to published data for the bulk refractive indices of the active region constituent quaternary alloys near 2.3 μm.[12] The linear fit in Fig. 1 is useful since it enables us to linearly extrapolate the λ^2_{CM} line to obtain λ_{CM} at normal incidence, which will be of use later in this study. As we increased θ and the E_{CM} blue shifted, we also observed that the normalised reflectivity spectra started to show changes in both the depth and shape of the CM dip profile (see Fig. 1, inset). The CM was observed to have the deepest, most symmetric dip, at $\sim$0.544 eV ($\sim$2.28 μm) at an incidence angle of 45 $\pm$ 5° (at RT). Such a condition is sometimes interpreted as being an indication that E_{CM} and E_{QW} are in alignment at this angle.[13] However, as discussed later, this initial finding is insufficient to draw this conclusion.

B. Temperature dependent reflectivity

Studying the PR spectra as a function of temperature can give more detailed information about the relative positions of E_{CM} and E_{QW}. Both energies increase with cooling. E_{QW} increases due to the variation of the fundamental band gap energy with temperature. Decreasing the temperature decreases the refractive index of the materials within the active region, as well as decreasing the average lattice constant, thus changing the cavity optical thickness, which determines the CM wavelength. Thus, E_{CM} will also increase with cooling but generally at a rather lower rate than E_{QW}.[10]

Figures 2(a) and 2(b) illustrate the normalised reflectivity spectra as a function of temperature between 9 K and 325 K, for samples A and B, respectively, at an incidence angle of 45°. An approximately linear increase of E_{CM} with cooling is observed at a rate of 0.043 $\pm$ 0.002 meV/K for both samples A and B, respectively (thick dashed lines in Fig. 2). The E_{CM} in Fig. 2(b) is of course only due to the bottom DBR, and is at a higher value of $\sim$0.57 eV (at 9 K) than the E_{CM} of sample A ($\sim$0.55 eV). As a helpful guide to the relative motions of the various features with temperature, Figs. 2(a) and 2(b) also show the positions of the QW ground-state transition energies E_{QW} (circles) as obtained from subsequent fits to the PR spectra, which will be discussed later. Note that the position of E_{QW} can also just be discerned as a slight dip in the R spectra of sample B, for instance, at 200 K, 225 K, and 250 K in Fig. 2(b). As can be seen, both the E_{QW} and E_{CM} energies blue-shift with cooling but E_{QW} shifts at a faster rate ($\sim$0.292 $\pm$ 0.006 meV/K between 150 and 300 K) than E_{CM}. In the PR of sample B we were also able to observe a QW higher-order transition (HOT), E_{HOT} at $\sim$0.58 eV (at 175 K) and, again as a helpful guide, the subsequent PR fitted energies for this are shown in Fig. 2(b) by the open squares.

Since E_{CM} decreases more slowly with increasing temperature than E_{QW}, and $E_{QW} > E_{CM}$ at 9 K, then E_{QW} may be made to cross over and be tuned into resonance with E_{CM} by heating from 9 K.[5,7,10] This may be observed in the temperature dependent PR measurements which were performed at the same time as the normalised reflectivity measurements of Fig. 2. Figure 3(a) shows the PR results for the full VCSEL

[This article is copyrighted as indicated in the article. Reuse of AIP content is subject to the terms at: http://scitation.aip.org/termsconditions. Downloaded to] IP: 164.67.194.158 On: Tue, 07 Jan 2014 22:58:43

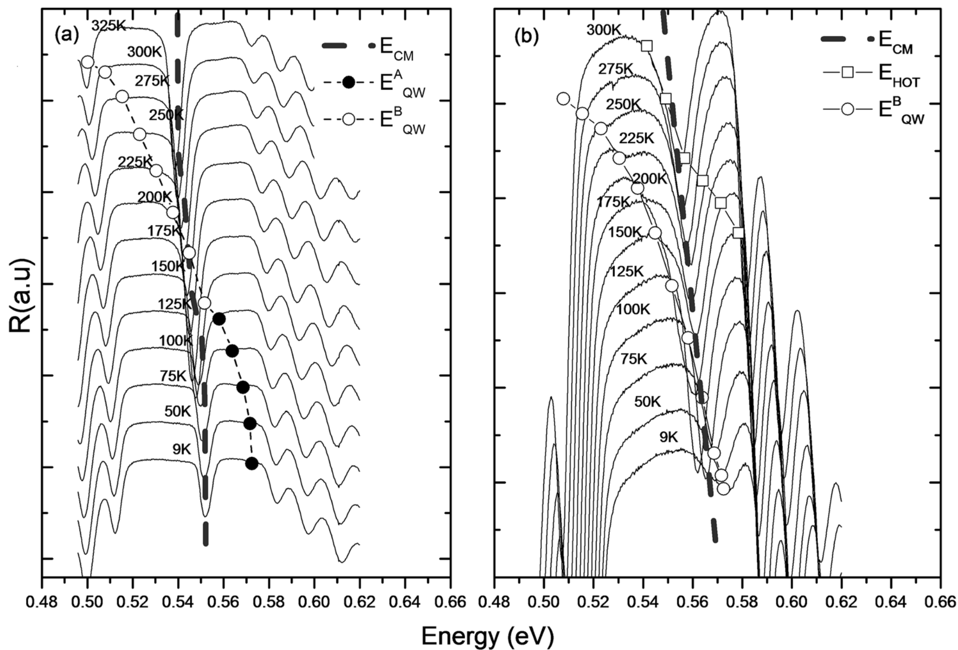

FIG. 2. Normalised reflectivity spectra for (a) sample A and (b) sample B, as a function of temperature, shown vertically offset for clarity. The angle of incidence is 45°. The position of the CM dip E_{CM} is shown by the thick dashed line. The circles show the E_{QW} values obtained from subsequent fits to the PR spectra for samples A (filled circles) and B (open circles). E_{CM} and E_{QW} both red shift with heating in both samples, but E_{CM} decreases more slowly than E_{QW}. The open squares show the position of the QW higher order transition energy, E_{HOT}, also obtained from later PR fits in sample B. E_{CM} (at 45° angle of incidence) and E_{QW} come into resonance at ~175 K and ~100 K for samples A and B, respectively.

structure sample A from 9 to 125 K. Figure 3(b) shows the corresponding PR spectra for the etched sample B, showing that good PR spectra were measurable from 9 to 300 K. The solid curves in both figures show the fitted spectral profiles using the model of Ref. 11 for Eq. (1). The PR spectra for sample A show a clear strong oscillatory feature associated with the CM dip (at ~0.55 eV at 9 K) whose movement is shown by the thick dashed line, and a weaker feature at higher energies (marked by filled circles) which we interpret as being due to the QW ground-state transition. Above 125 K this second feature became rather too weak to give reliable interpretations of the position of E_{QW}. In sample B the CM feature is less obvious in the PR spectra (thick dashed line), though we can observe two strong features (marked by open circles and squares) which we interpret as due to the QW ground-state transition and the higher-order QW transition, respectively. In contrast to sample A, we are able to measure clear PR spectra from sample B all the way from 9 K to RT with CM and QW features clearly observable (Fig. 3(b)), presumably due to the fact that the top DBR was removed, so allowing better penetration of the pump and probe light into the structure. At 9 K, a clear feature is observed at $E_{QW} \approx 0.57$ eV in both samples. In sample B, this energy then decreases with increasing temperature and overlaps with the CM feature at about 100 K at ~0.56 eV. At 175 K, the second QW transition E_{HOT} appears at ~0.58 eV in

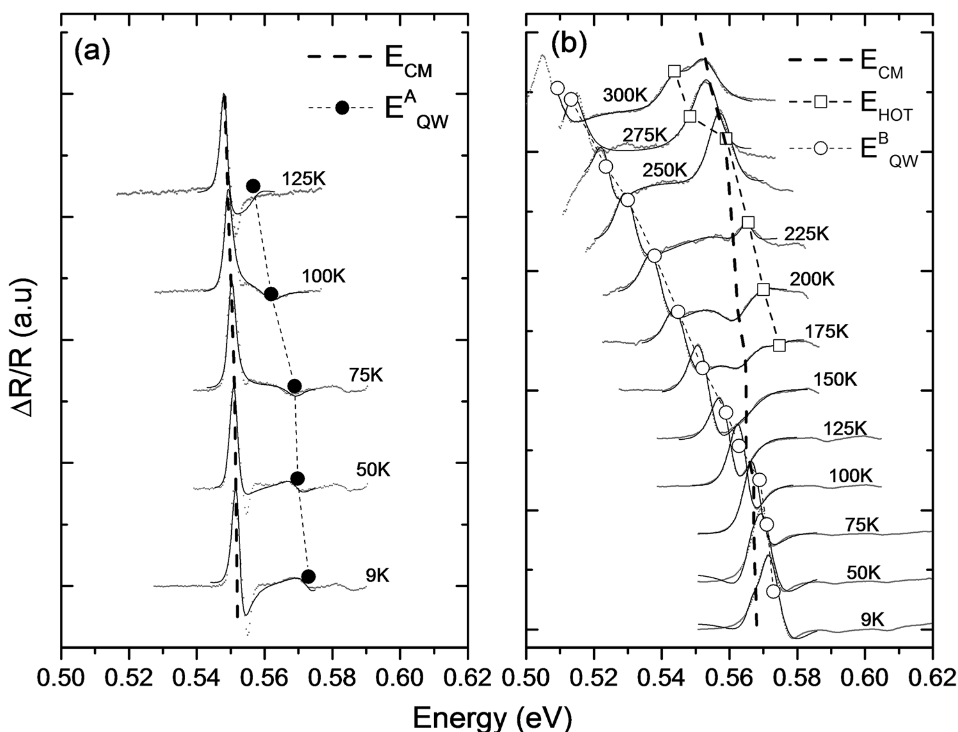

FIG. 3. The temperature dependent PR spectra of (a) sample A and (b) sample B at incidence angle 45°. For clarity, the spectra are offset vertically. The circles are a guide to the movement of E_{QW} in samples A (filled circles) and B (open circles), and the open squares are for E_{HOT} (sample B only). The movement of E_{CM} is shown by the thick dashed lines. The full curves are fits to the PR spectra with the model for VCSEL PR proposed in Ref. 11.

[This article is copyrighted as indicated in the article. Reuse of AIP content is subject to the terms at: http://scitation.aip.org/termsconditions. Downloaded to] IP: 164.67.194.158 On: Tue, 07 Jan 2014 22:58:43

sample B (open squares). This feature also moves progressively closer to E_{CM} and overlaps with, and crosses, it at ~250 K at ~0.57 eV in sample B.

Figure 4 summarises the results obtained here for the temperature dependence of the various fitted and measured energies. For the E_{CM} results of VCSEL sample A, those obtained from fitting the PR spectra are denoted by filled upward triangles, and are found to agree well with the filled downward triangles which are the E_{CM} values obtained directly from the normalised reflectivity spectra. The open upward triangles in Fig. 4 are the sample B E_{CM} results from the PR fits. All the PR spectra were measured at a 45° incidence angle but in Fig. 4 all the E_{CM} results have been extrapolated to normal incidence values using the aforementioned linear fit of Eq. (2) to the angle dependent normalised room temperature R spectra results (see Fig. 1). The lines passing through the E_{CM} results for both samples are linear fits giving slopes, as mentioned earlier, of 0.043 ± 0.002 meV/K in both samples A and B, respectively.

We may note from Fig. 4 that the sample B E_{CM} results lie at a somewhat higher energy than those of sample A—by ~15 meV. This discrepancy may in part be caused by the aforementioned 25 nm (~6 meV) blue-shift in the CM position between the wafer centre and edge, because sample A was measured at the centre of its wafer strip while sample B came from its wafer edge. The remainder of the ~15 meV discrepancy may have arisen from two other factors: first, since sample B has a missing top DBR then it is not a full VCSEL structure and consequently the CM dip is unlikely to occur at the same position as it would when the top DBR is present; second, the process of removing the top DBR from sample B by etching may have altered the observed E_{CM} position.

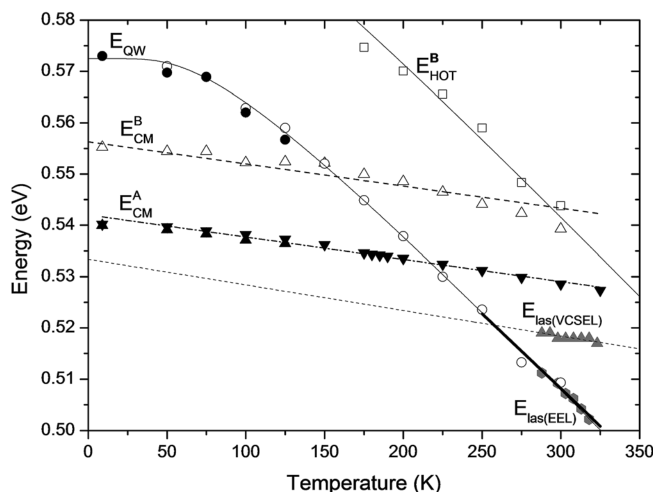

FIG. 4. Temperature dependence of E_{CM} for sample A (black filled, upward triangles from PR and downward triangles from R measurements) and sample B (open upward triangles from PR measurements), E_{QW} (filled circles for sample A, open circles for sample B) and E_{HOT} (open squares for sample B). The solid curves show fits to the E_{QW} and E_{HOT} data with the Bose-Einstein model, Eq. (3), while the E_{CM} data are shown fitted with straight lines. The symbols in grey lower right are the shifted emission energy results reported in Ref. 8 for operating VCSEL and EEL devices with the dashed and thick solid lines being linear fits to those results, respectively.

The circles in Fig. 4 represent the E_{QW} results: the filled circles are those obtained from fitting the PR spectra of sample A and the open circles are the corresponding fitted PR results from sample B. These are clearly in good agreement. The curve shown passing through these results is a fit with a Bose-Einstein model[14]

$$E = E_0 - 2\alpha_B/(e^{(\theta_B/T)} - 1), \quad (3)$$

giving a satisfactory agreement with the E_{QW} measurements and with fit parameters as follows: E_0, the band gap energy at $T = 0$, is 0.5725 ± 0.0008 eV; θ_B, the average phonon temperature, is 223 ± 19 K and α_B, the Bose-Einstein parameter, is 35 ± 4 meV. These θ_B and α_B values are close to other published Bose-Einstein parameters for similar GaInAsSb compositions.[15] The open squares in Fig. 4 show the results for E_{HOT} obtained from the fits to the PR spectra of sample B and the curve passing through these is the same Bose-Einstein fit as mentioned above, but shifted up by 35 meV. The other data in Fig. 4 (filled grey symbols, from device studies) will be discussed in Sec. IV C.

As may be seen from Fig. 4 the fitted lines through the E_{CM} and E_{QW} results for VCSEL sample A cross at a temperature of $\sim 220 \pm 2$ K and an energy of ~0.532 eV. Thus, the prediction from these PR studies is that neglecting temperature dependent recombination processes, the VCSEL will come into the ideal operating condition near this temperature with a lasing wavelength of ~2.33 μm. First, we note that this disagrees with the earlier tentative conclusion made from the variations in the depth of the CM dip in the RT angle-dependent studies of the reflectivity spectra mentioned earlier (Fig. 1, inset) where we observed a possible resonance between the CM and a QW transition at $\theta = 45 \pm 5°$. The results of Fig. 4 suggest that this RT angular resonance is in fact associated with the CM crossing the QW higher order transition rather than the ground-state transition; the E_{HOT} results in Fig. 4 and Eq. (2) together indicate that E_{CM} and E_{HOT} are equal at $\theta = 45°$ at RT. Second, we note that the predicted ideal operating temperature of ~220 K is well below the desired room temperature operation. An ideal VCSEL requires $E_{QW} > E_{CM}$ at 300 K, so that they would come into alignment when the operating device heats up due to the driving current. The PR studies show that in this VCSEL structure $E_{QW} = E_{CM}$ at $\sim 220 \pm 2$ K, and therefore that, in spite of the VCSELs operating at room temperature, the growth and device properties are not fully optimised.

C. Comparison of PR results with device studies

Given the above predictions for the VCSEL operation from our temperature-dependent R and PR results, we now turn to a comparison of this with the measurements of Ref. 8 on the lasing energies for actual operating VCSEL devices processed from the same wafer as sample A. In order to measure the behaviour of the QW emission energy, unaffected by the VCSEL DBRs, those device studies also investigated an edge-emitting laser (EEL) with nominally similar active region to the VCSEL. Figure 4 shows the results from Ref. 8 as filled grey symbols. The grey circles show the lasing

[This article is copyrighted as indicated in the article. Reuse of AIP content is subject to the terms at: http://scitation.aip.org/termsconditions. Downloaded to] IP: 164.67.194.158 On: Tue, 07 Jan 2014 22:58:43

energies of the operating EEL device $E_{las(EEL)}$, but red-shifted by ~36 meV. This offset was applied by those authors in order to give the same VCSEL E_{QW}/E_{CM} alignment temperature of −10 °C which was previously reported by Ref. 9, which may be justified if the active regions of the EEL and VCSEL devices were not actually identical. The grey triangles are the VCSEL lasing energy values $E_{las(VCSEL)}$ reported in Ref. 8. One would normally assume $E_{las(VCSEL)}$ is centred close to the CM dip energy, E_{CM}, of the operating VCSEL device (though, see later discussion). The $E_{las(VCSEL)}$ data are linearly fitted in Fig. 4 (dashed line) and, as can be seen, they increase with cooling at a rate of $dE_{las(VCSEL)}/dT = 0.05$ meV/K. As one might expect, this is close to the gradient observed for E_{CM} in sample A from the PR studies (0.043 ± 0.002 meV/K).

The red-shifted EEL emission energies (grey circles) were found to increase with cooling at a rate of $dE_{las(EEL)}/dT = 0.30$ meV/K, as shown by the solid line to the lower right in Fig. 4. Reference 8 made the assumption from Ref. 9 that the minimum threshold current was at −10 °C and therefore argued that E_{QW} and E_{CM} come into resonance in the operating VCSEL device at ~263 K and 2.38 μm (i.e., where the dashed and solid lines cross in the lower right of Fig. 4), and that, at RT, the CM is detuned by ~+10 meV from the QW gain peak in the VCSEL device.

Figure 4 allows us to compare the results from the present PR study with the device results. If the argument of Ref. 8 for red-shifting their $E_{las(EEL)}$ measurements is correct then these data should lie close to the present measured QW ground-state transition energy E_{QW}. It may be seen that our PR measurements of E_{QW} are indeed consistent with the red-shifted $E_{las(EEL)}$ plot of Ref. 8, the two temperature behaviours overlapping satisfactorily (i.e., our Bose-Einstein fit to E_{QW}, when extrapolated to higher temperatures, merges well with the linear fit to $E_{las(EEL)}$). However, our E_{CM} results for sample A are significantly higher than the $E_{las(VCSEL)}$ values reported by Ref. 8—by some 10 meV. As a result, the resonance temperature indicated by the PR results (220 ± 2 K) is significantly lower than that suggested by the device results (~263 K). Also, the PR studies show that the detuning between E_{QW} and E_{CM} at RT (~21 meV) is larger than that suggested by the device studies (~10 meV) of Ref. 8. The possible reasons behind this discrepancy are discussed next.

We considered the possibility that the observed difference between the PR and device results in the resonance temperature for the VCSEL (caused primarily by the higher E_{CM} values observed in the PR studies as compared to the device studies) might arise from the post-growth annealing used in processing the VCSEL wafer structure into a full device in Ref. 8; the annealing technique might have caused changes in the E_{CM} and/or the E_{QW} of the processed device.

To further explore this possibility, a piece from the edge of the sample A VCSEL wafer strip was cleaved off and annealed using the same technique and conditions as Ref. 8. A reflectivity measurement at RT was then performed. Figure 5 gives a comparison of the normalised normal-incidence reflectivity spectra before and after annealing. As can be seen, the annealing has caused a small red-shift in the CM dip position of ~3 meV (12 nm) from 0.534 eV (2320 nm) to 0.531 eV (2332 nm) but the main effect is to considerably broaden the CM dip. Although the shift of 3 meV is not sufficient in itself to account for the apparent 10 meV difference between E_{CM} and $E_{las(VCSEL)}$ found in Fig. 4, the broader CM would have a pronounced effect on the spectral distribution of light leaving the device. In an ideal VCSEL, efficient lasing will only occur near the minimum of a sharply defined CM dip when it overlaps with the QW gain peak. A broadened CM dip would allow a range of QW spectral emission to escape, the spectrum of which would result from a convolution of the QW gain spectrum and reflectivity CM profile, which may not necessarily peak at the lowest point of the CM dip. Referring to Fig. 5, at RT the PR measured E_{QW} energy is at ~0.51 eV, lying to the left of the centre of the CM dip of the annealed sample, while the emission peak $E_{las(VCSEL)}$ lies somewhat closer to the CM dip at 0.52 eV. We conclude, therefore, that the convolution of the QW gain spectrum peaking around E_{QW} and the broad VCSEL CM dip produces a lasing peak somewhat towards the lower energy side of the CM dip in the annealed VCSEL, at the position shown in Fig. 5 for $E_{las(VCSEL)}$ given by Ref. 8. In these circumstances, the measurements of $E_{las(VCSEL)}$ by Ref. 8 might not be centred on E_{CM} due to the influence of this annealing, and it is too simplistic to assume that the observed VCSEL device lasing energy is equal to the position of the CM dip minimum in the VCSEL structure. We note that other factors influence the lasing wavelength of the VCSEL devices, including band filling, particularly under high pumping conditions due to the presence of non-radiative recombination,[6] as may be expected in devices operating at longer wavelengths.

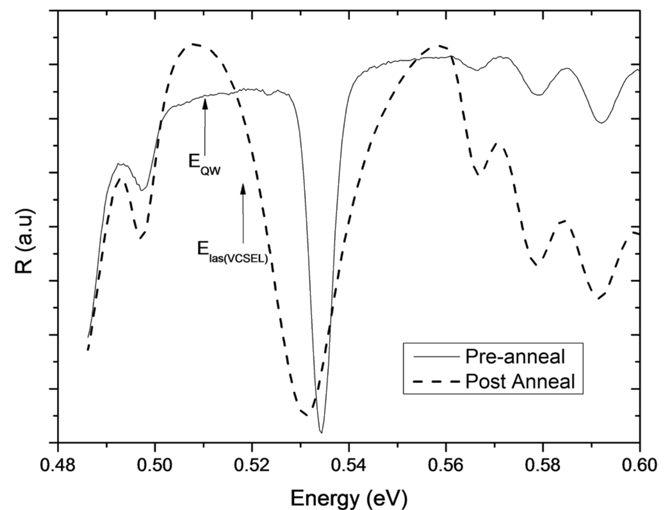

FIG. 5. Normal incidence room temperature reflectivity measurements on a pre-annealed (solid curve) and post-annealed (dashed curve) piece of the sample A VCSEL wafer strip. The CM dip is broadened after annealing and slightly red-shifted. The arrows show the E_{QW} transition energy determined by PR and the lasing energy of the operating VCSEL $E_{las(VCSEL)}$ reported in Ref. 8.

V. SUMMARY AND CONCLUSIONS

We have made a detailed spectroscopic characterization of pre-fabrication 2.3 μm GaSb-based VCSEL wafer

[This article is copyrighted as indicated in the article. Reuse of AIP content is subject to the terms at: http://scitation.aip.org/termsconditions. Downloaded to] IP: 164.67.194.158 On: Tue, 07 Jan 2014 22:58:43

samples, at temperatures ranging from 9 K to 300 K. Angle dependent reflectivity measurements allowed us to extrapolate our subsequent temperature variation results (performed at an incidence angle of 45°) to the normal incidence condition. The temperature dependent PR spectra clearly showed features associated with not only the CM dip, but also several QW transitions. Fitting our PR with an appropriate lineshape model yielded two QW transition energies, E_{QW} and E_{HOT}, as a function of temperature. At room temperature, it was found that the CM dip occurs at the desired emission wavelength, ~0.52 eV (~2.35 μm). However, we found that the QW ground-state transition energy is not aligned with the CM dip at this temperature and is some 21 meV below it. However, the two features could be brought into alignment at energy of ~0.53 eV (2.35 μm) by cooling to 220 ± 2 K. Our results for the ground-state transition energy E_{QW} are in good agreement with the conclusions of a separate temperature-dependent study of the emission energy of edge-emitting laser devices with a similar active region to the VCSEL.[8] That study also measured the lasing energy of a VCSEL fabricated from the same wafer as in the present study. Comparing this with the present PR results suggested that the E_{CM} energy in the processed device is some 10 meV lower than determined in our PR studies. This has the consequence that E_{CM} and E_{QW} are predicted to come into resonance in the operating VCSEL at a higher temperature in the region of ~263 K compared to our PR result of 220 K. We investigated the likely causes for this disagreement and demonstrated that the annealing process used in Ref. 8 to fabricate the VCSELs results in a red-shift and broadening of the CM dip in the processed device. We concluded, therefore, that the convolution of this broadened CM dip and QW gain spectrum may contribute to a lowering of the emission energy. Furthermore, this VCSEL emission energy does not truly reflect the position of the centre of the CM dip in the processed device, and lies somewhat below the actual E_{CM}. Thus, one should be wary of interpreting the emission energy of a VCSEL device as a measure of the energy position of E_{CM}.

To conclude, the utility of the PR characterisation technique has been clearly demonstrated for these VCSEL structures; to date, it is the only known non-destructive optical technique that can monitor the QW transition energies in full VCSEL structures. The study amply demonstrates the usefulness of PR for non-destructive pre-fabrication optical characterisation in VCSEL manufacturing, especially the degree of alignment between the QW gain peak and the cavity dip, and the temperature at which they can be brought into resonance, a condition of vital importance for the efficient and successful operation of VCSEL devices.

ACKNOWLEDGMENTS

We acknowledge funding provided by the following: "Malaysian University Grant Program (GUP) Tier 1," Universiti Teknologi Malaysia and M.O.H.E. (Grant Nos. Q.J130000.7126.01H55 and Q.J130000.7126.4D031); U.T.M. Zamalah Ph.D. scholarship for G. M. T. Chai; Engineering and Physical Sciences Research Council (EPSRC) (UK) and QinetiQ for funding for N. E. Fox; Petroleum Technology Development Fund (Nigeria) for a studentship for A. B. Ikyo; and EPSRC(UK) grants (Nos. EP/H005587/1 and GR/064725/01).

[1]J. Bengtsson, J. Gustavsson, Å. Haglund, A. Larsson, A. Bachmann, K. Kashani-Shirazi, and M.-C. Amann, Opt. Express **16**(25), 20789–20802 (2008).
[2]A. D. L. Cerutti, G. Narcy, P. Grech, G. Boissier, A. Garnache, E. Tournié, and F. Genty, J. Cryst. Growth **311**(7), 1912–1916 (2009).
[3]A. Bachmann, K. Kashani-Shirazi, S. Arafin, and M. C. Amann, IEEE J. Sel. Top. Quantum Electron. **15**(3), 933–940 (2009).
[4]P. Vicente, P. Thomas, D. Lancefield, T. Sale, T. J. C. Hosea, A. Adams, P. Klar, and A. Raymond, Phys. Status Solidi B **211**(1), 255–262 (1999).
[5]G. Blume, K. Hild, I. P. Marko, T. J. C. Hosea, S. Q. Yu, S. A. Chaparro, N. Samal, S. R. Johnson, Y. H. Zhang, and S. J. Sweeney, J. Appl. Phys. **112**(3), 033108 (2012).
[6]K. Hild, I. P. Marko, S. R. Johnson, S. Q. Yu, Y. H. Zhang, and S. J. Sweeney, Appl. Phys. Lett. **99**(7), 071110 (2011).
[7]T. J. C. Hosea, Thin Solid Films **450**(1), 3–13 (2004).
[8]A. B. Ikyo, I. P. Marko, A. R. Adams, S. J. Sweeney, A. Bachmann, K. Kashani-Shirazi, and M. C. Amann, IET Optoelectron. **3**(6), 305–309 (2009).
[9]A. Bachmann, T. Lim, K. Kashani-Shirazi, O. Dier, C. Lauer, and M.-C. Amann, Electron. Lett. **44**(3), 202–203 (2008).
[10]S. A. Cripps, T. J. C. Hosea, S. J. Sweeney, D. Lock, T. Leinonen, J. Lyytikainen, and M. Dumitrescu, IEE Proc. – Optoelectron. **152**(2), 103–109 (2005).
[11]S. A. Cripps and T. J. C. Hosea, Phys. Status Solidi A **204**(2), 331–342 (2007).
[12]S. Adachi, J. Appl. Phys. **61**(10), 4869–4876 (1987).
[13]S. A. Cripps, Ph.D. thesis, University of Surrey, 2007.
[14]K. P. O'Donnell and X. Chen, Appl. Phys. Lett. **58**(25), 2924–2926 (1991).
[15]M. Muñoz, F. H. Pollak, M. Zakia, N. Patel, and J. Herrera-Perez, Phys. Rev. B **62**(24), 16600 (2000).

[This article is copyrighted as indicated in the article. Reuse of AIP content is subject to the terms at: http://scitation.aip.org/termsconditions. Downloaded to] IP: 164.67.194.158 On: Tue, 07 Jan 2014 22:58:43